

Suzaku view of Be/X-ray binary pulsar GX 304-1 during Type I X-ray outbursts

Gaurava K. Jaisawal^{*}, Sachindra Naik[†] and Prahlad Epili[‡]

Astronomy and Astrophysics Division, Physical Research Laboratory, Navrangapura, Ahmedabad - 380009, Gujarat, India

ABSTRACT

We report the timing and spectral properties of Be/X-ray binary pulsar GX 304-1 by using two *Suzaku* observations during its 2010 August and 2012 January X-ray outbursts. Pulsations at ~ 275 s were clearly detected in the light curves from both the observations. Pulse profiles were found to be strongly energy-dependent. During 2010 observation, prominent dips seen in soft X-ray (≤ 10 keV) pulse profiles were found to be absent at higher energies. However, during 2012 observation, the pulse profiles were complex due to the presence of several dips. Significant changes in the shape of the pulse profiles were detected at high energies (> 35 keV). A phase shift of ~ 0.3 was detected while comparing the phase of main dip in pulse profiles below and above ~ 35 keV. Broad-band energy spectrum of pulsar was well described by a partially absorbed Negative and Positive power-law with Exponential cutoff (NPEX) model with 6.4 keV iron line and a cyclotron absorption feature. Energy of cyclotron absorption line was found to be ~ 53 and 50 keV for 2010 and 2012 observations, respectively, indicating a marginal positive dependence on source luminosity. Based on the results obtained from phase-resolved spectroscopy, the absorption dips in the pulse profiles can be interpreted as due to the presence of additional matter at same phases. Observed positive correlation between cyclotron line energy and luminosity, and significant pulse-phase variation of cyclotron parameters are discussed in the perspective of theoretical models on cyclotron absorption line in X-ray pulsars.

Key words: pulsars: individual (GX 304-1) – stars: neutron – X-rays: stars

1 INTRODUCTION

Be/X-ray binary pulsar GX 304-1 was discovered during hard X-ray sky surveys with balloon observations in 1967 (McClintock et al. 1971). The X-ray source was detected with successive space missions and recognized as 3U 1258-61, 4U 1258-61 & 2S 1258-613 (Giacconi et al. 1974; Bradt et al. 1977; Forman et al. 1978). Using data from *SAS* – 3 observations, X-ray pulsations at ~ 272 s were discovered in the source (McClintock et al. 1977). Spectral investigation of the pulsar, carried out from balloon observations, showed that the continuum spectrum in 18-35 keV range was described by a power-law (Maurer et al. 1982). Later, a power-law model modified with high energy cutoff was used to explain the 2-40 keV continuum spectrum obtained from *HEAO* 1 observation of the pulsar (White, Swank & Holt 1983). Analyzing the periodicity of the X-ray outbursts in 7 years of

data from *Vela* 5B, the orbital period of the GX 304-1 was reported to be 132.5 d (Priedhorsky & Terrell 1983). A shell star with visual magnitude of 15 was discovered in the X-ray error box of the neutron star and identified as the optical companion of the pulsar (Mason et al. 1978). High resolution optical spectroscopy established the spectral class of the companion as Be star of type B2 Vne which is at a distance of 2.4 ± 0.5 kpc (Parkes et al. 1980).

GX 304-1 was monitored with *EXOSAT* covering a duration of an expected outburst in 1984 July/August (Pietsch et al. 1986). However, no X-ray outburst was detected during the *EXOSAT* monitoring campaign. In contrast, the source flux was estimated to be significantly low e.g. by a factor of 25, than the quiescent flux level. This observed peculiarity was characterized as the X-ray “off” state of the pulsar. Long term optical monitoring of the Be companion star in 1978-1988 suggested a major change (loss) in the Be envelop or circumstellar disk, the consequence of which is considered as the possible cause of the X-ray “off” state in

^{*} gaurava@prl.res.in

[†] snaik@prl.res.in

[‡] prahlad@prl.res.in

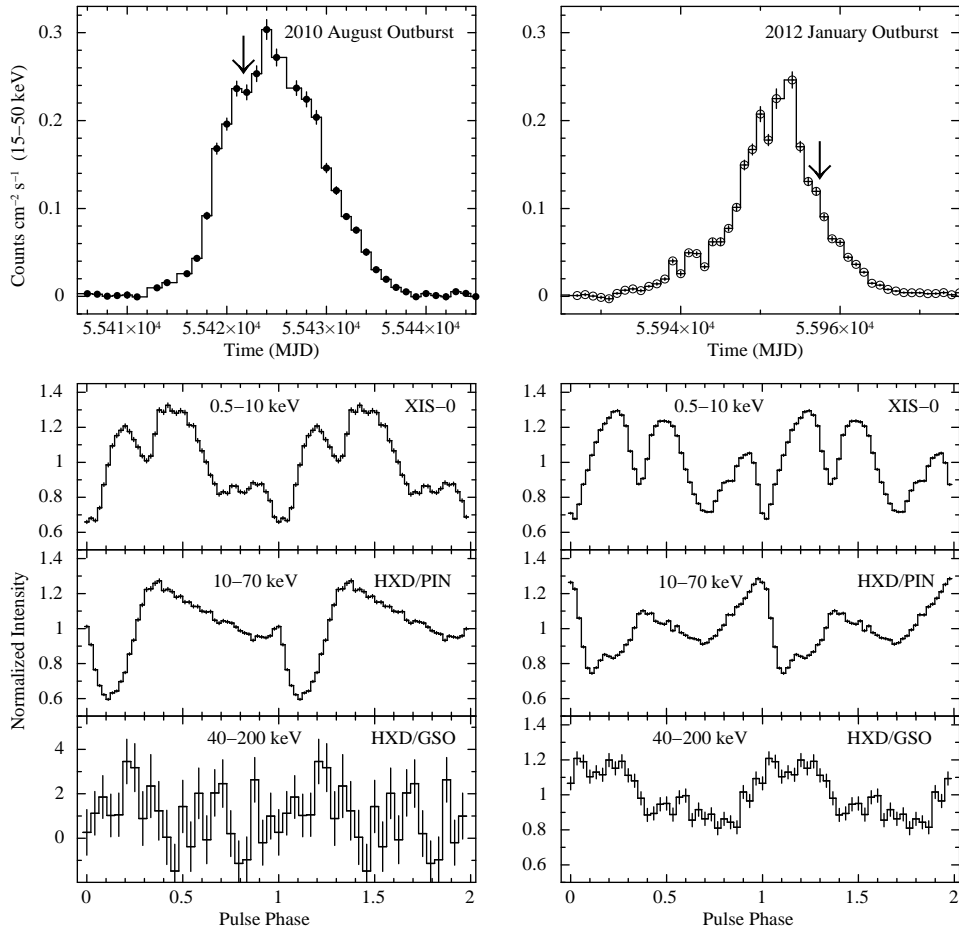


Figure 1. *Swift*/BAT light curves of GX 304-1 in the 15-50 keV energy band, from 2010 July 28 (MJD 55405) to 2010 September 06 (MJD 55445) and 2011 December 30 (MJD 55925) to 2012 February 18 (MJD 55975) are shown in both sides of first panel, respectively. The arrow marks in both sides of first panel shows the date of *Suzaku* observations of GX 304-1 during outburst. Corresponding pulse profiles in 0.5-10 keV (XIS-0; second panel), 10-70 keV (PIN; third panel) and 40-200 keV (GSO; fourth panel) obtained from the background subtracted light curves of both the observations are shown in both sides of figure. Phase zero was arbitrarily chosen at MJD 55421.76 and 55957.4326 for first and second observations, respectively. The errors in the pulse profiles are estimated for 1σ confidence level and two pulses are shown for clarity.

GX 304-1 (Corbet et al. 1986; Pietsch et al. 1986; Haefner 1988).

After 28 years of quiescence, an X-ray outburst was detected from GX 304-1 with the *INTEGRAL* observatory in 2008 June (Manousakis et al. 2008) after which the source was found to be active in X-rays. Since then, several X-ray outbursts have been detected in the pulsar with *Swift*/BAT and *MAXI* (Yamamoto et al. 2009, 2012; Krimm et al. 2010; Mihara et al. 2010). Using the *Rossi X-Ray Timing Explorer* (*RXTE*) observations during 2010 August outburst, energy and luminosity dependence of pulse profiles were found in GX 304-1 (Devasia et al. 2011). Apart from the evolution of pulse profiles, a quasi-periodic oscillation (QPO) at ~ 0.125 Hz was detected with harmonics in several *RXTE*/PCA observations during this outburst. The pulsar spectrum in 3-30 keV range was described with a partial covering high energy cutoff power-law model (Devasia et al. 2011). During the same outburst in 2010 August, a cyclotron absorption feature at ~ 54 keV was detected in the pulsar spectrum (Yamamoto et al. 2011) and the corresponding magnetic field of the neutron star was estimated to be

$\sim 4.7 \times 10^{12}$ G. A positive correlation between cyclotron energy and luminosity was seen during 2012 January-February outburst with *INTEGRAL* (Klochkov et al. 2012). Malacaria et al. (2015) performed timing and spectral analysis of the pulsar using the same *INTEGRAL* data. The shape of the pulse profiles obtained from these observations were found to be similar in 20-40 keV, 40-60 keV and 18-80 keV energy ranges. Phase-resolved spectroscopy was carried out by stacking multiple spectra of different fluxes. From this analysis, the cyclotron absorption line energy was found to be nearly constant (within errors) with pulse phases, except about 10% variation at one phase bin (Malacaria et al. 2015). The evolution of the pulse period with luminosity was studied by using data from *MAXI*/GSC, *RXTE*/PCA, *Swift*/XRT and *Fermi*/GBM observations during a series of outbursts from 2009 to 2013 (Postnov et al. 2015; Sugizaki et al. 2015). The observed pulse period variation was interpreted in terms of binary modulation along with the spinning-up of the neutron star. The orbital parameters of the binary system were estimated to be – orbital period = 132.19 d, epoch at the periastron = MJD 55425, pulse

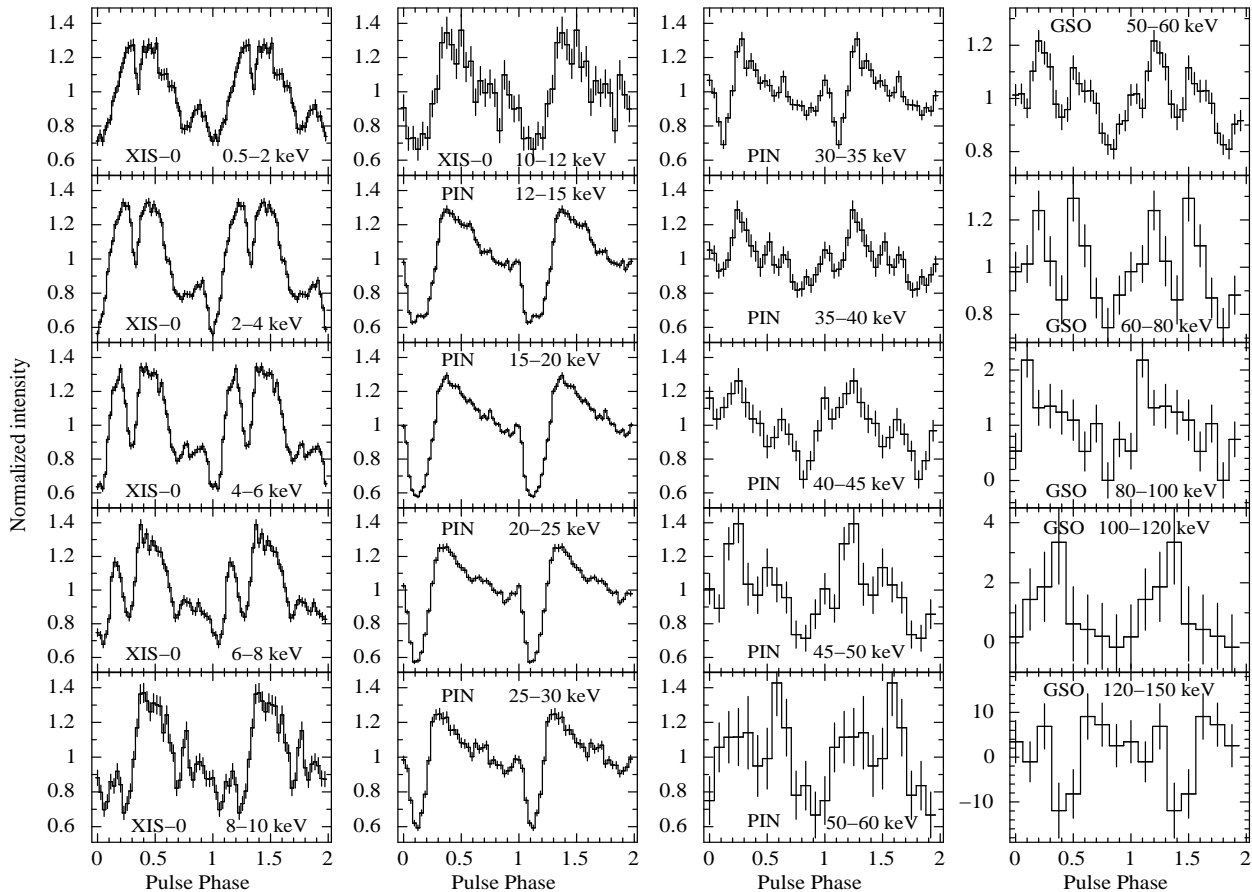


Figure 2. Energy-resolved pulse profiles of GX 304-1 obtained from XIS-0, HXD/PIN and HXD/GSO light curves at various energy ranges, during first *Suzaku* observation in 2010 August outburst. The presence of absorption dips in profiles can be seen at various pulse phases. The error bars represent 1σ uncertainties. Two pulses in each panel are shown for clarity.

period $\simeq 275.45$ s, orbital eccentricity $\simeq 0.5$, $a_r \sin i \simeq 500$ – 600 light-s and ω at periastron $\simeq 122.5^\circ$ – 130° (Sugizaki et al. 2015).

In this work, the timing and broad-band spectral properties of GX 304-1 were presented in detail by using two *Suzaku* observations during its outbursts in 2010 August and 2012 January. Earlier, the evolution of pulse profiles up to ~ 30 keV had been reported by using *RXTE*/PCA observations during 2010 outburst (Devasia et al. 2011). Using *Suzaku* observations, the evolution of pulse profiles up to ~ 150 keV has been presented in this paper. The observed changes in the shape of pulse profiles close to the cyclotron absorption line are also being discussed. Although spectral studies of the pulsar during its 2012 outburst has been reported in 5–100 keV range by using *INTEGRAL* observations (Malacaria et al. 2015), *Suzaku* observations provide a better opportunity to investigate a detailed spectral and timing study in broad energy range (1–150 keV). The details of observations, data analysis, results and interpretations are described in following sections of the paper.

2 OBSERVATION AND ANALYSIS

Suzaku, the fifth Japanese X-ray mission, was launched by Japan Aerospace Exploration Agency (JAXA) on 2005 July 10 (Mitsuda et al. 2007). It offers a broad energy coverage

(0.2–600 keV) in the electromagnetic spectrum by using two sets of instruments e.g. the X-ray Imaging Spectrometers (XIS; Koyama et al. 2007) and Hard X-ray Detectors (HXD; Takahashi et al. 2007). The XISs are imaging CCD cameras and cover 0.2–12 keV energy range. Among four XISs, three XISs (XIS-0, XIS-2, XIS-3) are front-illuminated whereas one XIS (XIS-1) is back-illuminated. The effective areas of front and back-illuminated XISs are 340 cm^2 and 390 cm^2 at 1.5 keV, respectively. Field of view of XIS detectors is $18' \times 18'$ in full window mode. The HXD unit of *Suzaku* consists of two sets of detectors such as HXD/PIN and HXD/GSO. HXD/PIN is a silicon diode detector covering 10–70 keV energy range, whereas HXD/GSO is a crystal scintillator detector working in 40–600 keV energy range. Effective areas for HXD/PIN and HXD/GSO are 145 cm^2 at 15 keV and 315 cm^2 at 100 keV, respectively. Field of view of HXD/PIN and HXD/GSO (up to 100 keV) is $34' \times 34'$.

GX 304-1 was observed with *Suzaku* during its outbursts in 2010 August and 2012 January. *Swift*/BAT light curves of the pulsar in 15–50 keV range, covering the outbursts are shown in top panels of Fig. 1. Arrow marks in both panels indicate the date of *Suzaku* observation of GX 304-1 during respective outbursts. During 2010 August outburst, the *Suzaku* observation was carried out at the peak of outburst whereas the second observation was made during the decay phase of the 2012 January outburst. The first observation

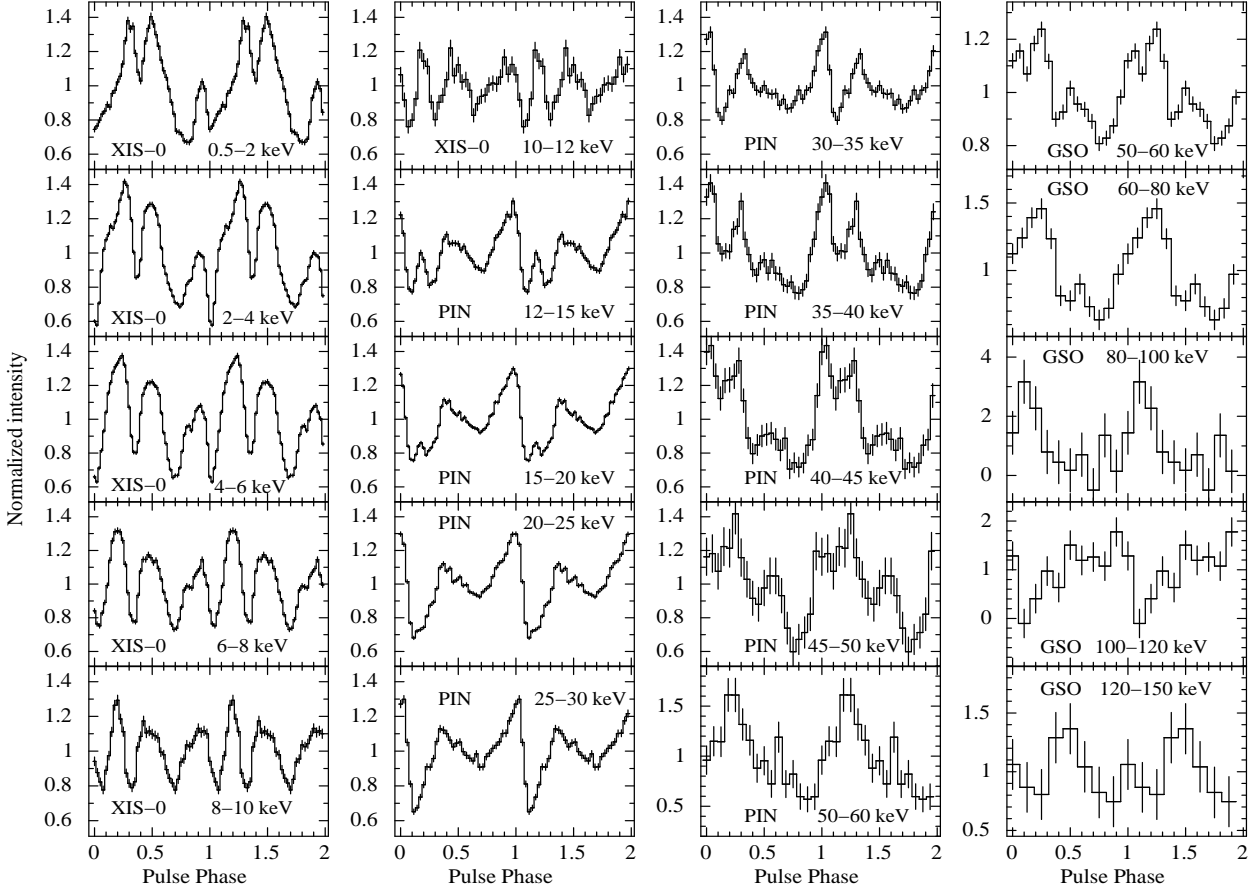


Figure 3. Energy-resolved pulse profiles of GX 304-1 obtained from XIS-0, HXD/PIN and HXD/GSO light curves at various energy ranges, during second *Suzaku* observation in 2012 January outburst. The presence of absorption dips in profiles at higher energies can be seen at various pulse phases. The error bars represent 1σ uncertainties. Two pulses in each panel are shown for clarity.

was performed on 2010 August 13, in ‘HXD nominal’ position with an effective exposure of ~ 5.1 ks and ~ 12.9 ks for XIS and HXD detectors, respectively. However, the second observation was made during 2012 January 31–February 02 for a longer effective exposures of ~ 16.5 ks for XIS and ~ 58.7 ks for HXD. The second observation was performed in ‘XIS nominal’ position. During both observations, the XIS detectors were operated in “burst” clock mode with ‘1/4’ window option yielding 0.5 s time resolution. The publicly available archival data (observation IDs: 905002010 and 406060010) were used in the present study. Heasoft software package of version 6.12 and calibration database (CALDB) for XIS and HXD released on 2014 February 03 and 2011 September 13, respectively, were used in the data analysis.

The unfiltered event data files were reprocessed by applying the ‘aepipeline’ package of FTOOLS. The clean event files generated after the reprocessing of XIS and HXD unfiltered event data were used in our analysis. The arrival times of the X-ray photons recorded in XIS and HXD event data were corrected for solar system barycenter by applying ‘aebarycen’ task of FTOOLS. The light curves and spectra of the pulsar were extracted from clean event data by using the *XSELECT* package of FTOOLS. The XIS event data were corrected for the effect of thermal flexing and wobbling

by applying attitude correction script *aeattcor.sl*¹. Subsequently, the pile-up estimation was made for XISs data by using S-lang script *pile_estimate.sl*². For first observation, a pile-up of $\sim 22\%$, $\sim 18\%$ and $\sim 28\%$ was found at the centers of XIS-0, XIS-1 and XIS-3, respectively. Therefore, an annulus region with inner and outer radii of $60''$ and $180''$ was selected to reduce the effect of pile-up to $\leq 4\%$. During the second observation, the pile-up was estimated to be 17%, 13% and 18% at the centers of XIS-0, XIS-1 and XIS-3, respectively. An annular region with $40''$ inner and $180''$ outer radii was used to reduce the pile-up effect to $\leq 4\%$ for the second observation. These annulus regions were used for the extraction of source light curves and spectra from cleaned XIS event data. The XIS background light curves and spectra were extracted from the event data by selecting a circular region away from the source. Response matrices and effective area files for XISs were created by using ‘xismfgen’ and ‘xissimarfgen’ tasks of FTOOLS, respectively. HXD being a non-imaging detector system, source light curves and spectra were obtained from cleaned HXD/PIN and HXD/GSO event data by using *XSELECT* package. However, PIN and GSO background light curves and spectra were accumulated from simulated non-X-ray background event files provided

¹ <http://space.mit.edu/ASC/software/suzaku/aeattcor.sl>

² http://space.mit.edu/ASC/software/suzaku/pile_estimate.sl

by the instrument team. A correction for cosmic X-ray background (CXB³) was also applied to PIN spectrum. In our spectral analysis, HXD/PIN response files released in 2010 July and 2011 June were used for 2010 August and 2012 January observations, respectively. For GSO data, response and effective area files released in 2010 May were used for 2010 August observations.

3 RESULTS

3.1 Timing Analysis

As described above, source and background light curves with 1 s time resolution were extracted from barycentric corrected XIS-0, PIN and GSO event data for both the observations. The χ^2 -maximization technique was used to estimate the pulse period of the pulsar. Pulsations at periods of 275.45 ± 0.05 and 274.88 ± 0.01 s were detected in the source light curves obtained from the first and second *Suzaku* observations, respectively. Quoted errors in pulse period are calculated for 90% confidence level. The estimated pulse periods were used to generate pulse profiles from background subtracted light curves from corresponding observations. Pulse profiles in 0.5-10 keV (XIS-0), 10-70 keV (PIN) and 40-200 keV (GSO) energy ranges for both the observations are shown in second, third and fourth panels of Fig. 1, respectively. Pulse profiles were generated by using 55421.7600 MJD as epoch (phase zero) for the first observation where as 55957.4326 MJD was used for the second observation.

Strong energy dependence of pulse profiles can be clearly seen during both observations (Fig. 1). Absorption dips at certain phases were seen in the soft X-ray pulse profiles (0.5-10 keV range). However, these dips disappeared from the pulse profiles in 10-70 keV range. The pulsations were absent or marginally seen in 40-200 keV pulse profiles obtained from GSO light curves. Apart from the energy dependence, the pulse profiles are also found to be luminosity dependent. The top panels of the Fig. 1 show that the *Suzaku* observations of the pulsar were carried out at different luminosity levels e.g. the source was comparatively brighter during the 2010 August observation than the 2012 January observation. However, the shape of the pulse profiles in soft and hard X-rays (second and third panels) are different due to the presence of absorption dips or dip-like features. Along with the energy and luminosity dependence of the pulse profiles in GX 304-1, a phase shift of ~ 0.1 (see Fig. 1) was also found between the soft (XIS) and hard (PIN) X-ray pulse profiles obtained from both the observations.

To investigate the evolution of pulse profiles with energy during both *Suzaku* observations, we generated energy resolved pulse profiles in various energy bands and are shown in Fig. 2 & 3 for first and second observations, respectively. It can be seen from Fig. 2 that a prominent and narrow absorption dip was present in pulse profiles up to ~ 8 keV. Beyond this energy, the peak in the pulse profiles prior to the dip (≤ 0.3 phase; left panels of Fig. 2) disappeared and broadened the minima in the pulse profile to 0.05-0.25 pulse

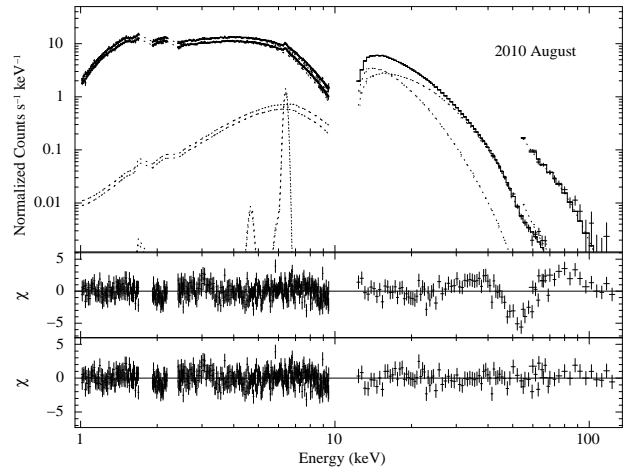


Figure 4. Energy spectrum of GX 304-1 in 1-130 keV energy range obtained with the XIS-0, XIS-3, PIN and GSO detectors from the first *Suzaku* observation in 2010 August outburst, along with the best-fit model comprising a partial covering NPEX continuum model, a Gaussian function for iron emission line and a cyclotron absorption component. The middle and bottom panels show the contributions of the residuals to χ^2 for each energy bin for the partial covering NPEX continuum model without and with cyclotron component in the model, respectively.

phase range (panels in second column of Fig. 2). We suggest that this broadening of the minima in the pulse profile is the possible cause of observed ~ 0.1 phase shift in the soft (0.5-10 keV) and hard X-ray (10-70 keV) pulse profiles. A careful inspection of Fig. 2 & 3 showed that the pulse profiles were complex due to presence of several absorption features (dips) at various pulse phases and strongly energy dependent up to ~ 12 keV beyond which the shape of the profiles became simple up to ~ 35 keV. The main dip in the pulse profiles in this energy range (12-35 keV) was observed to be phase-shifted by ~ 0.1 phase compared to that in soft X-ray profiles. In pulse profiles beyond ~ 35 keV, the main dip at ~ 0.1 phase appeared to be filled-up gradually with increase in energy. Along with the increase in the normalized intensity at ~ 0.1 phase (Fig. 2 & 3), a significant decrease in intensity was observed at ~ 0.7 - 0.8 phase range which appeared as the main dip in hard X-ray pulse profiles. These hard X-ray pulse profiles (≥ 40 keV) appeared to be single-peaked and pulsations were detected up to ~ 120 keV.

The energy resolved pulse profiles of GX 304-1 were found to be complex during both the *Suzaku* observations. Presence of multiple narrow and prominent absorption dips were seen up to as high as ~ 50 keV. Beyond this energy, the profiles appeared relatively simple. Presence of prominent dips up to higher energies and sudden change in phase of main dip in pulse profiles beyond ~ 35 keV made it interesting to investigate the properties of pulsar through phase-averaged and phase-resolved spectroscopy.

3.2 Spectral Analysis

3.2.1 Pulse-phase-averaged spectroscopy

Phase-averaged spectroscopy was performed by using spectra accumulated from XIS-0, XIS-1, XIS-3, PIN and GSO data obtained from both the observations. Earlier described

³ http://heasarc.nasa.gov/docs/suzaku/analysis/pin_cxb.html

Table 1. Best-fitting parameters (with 90% errors) obtained from the spectral fitting of *Suzaku* observations of GX 304-1 during 2010 August and 2012 January outbursts. Model-1 : partial covering NPEX model with Gaussian component; Model-2 : partial covering NPEX model with Gaussian component and cyclotron absorption line.

| Parameter | 2010 August | | 2012 January | |
|--------------------------------|-----------------|---------------------|-----------------|---------------------|
| | Model-1 | Model-2 | Model-1 | Model-2 |
| N_{H1}^a | 1.04 ± 0.02 | 1.02 ± 0.02 | 0.98 ± 0.02 | 0.97 ± 0.02 |
| N_{H2}^b | 13.2 ± 1 | 13.7 ± 1.2 | 5.7 ± 0.5 | 5.3 ± 0.5 |
| Cov. fraction | 0.35 ± 0.02 | 0.32 ± 0.02 | 0.25 ± 0.02 | 0.23 ± 0.02 |
| Photon index | 0.6 ± 0.03 | 0.57 ± 0.03 | 0.42 ± 0.02 | 0.43 ± 0.02 |
| E_{cut} (keV) | 6.6 ± 0.1 | 7.1 ± 0.2 | 6.8 ± 0.1 | 7.4 ± 0.2 |
| Fe line energy (keV) | 6.41 ± 0.02 | 6.41 ± 0.02 | 6.41 ± 0.01 | 6.41 ± 0.01 |
| Eq. width of Fe line (eV) | 44 ± 7 | 43 ± 8 | 23 ± 2 | 23 ± 3 |
| Cyclotron line energy (keV) | — | 53.2 ± 0.8 | — | 50 ± 1 |
| Width of cyclotron line (keV) | — | $6.5^{+2.1}_{-1.6}$ | — | $5.5^{+2.6}_{-1.8}$ |
| Depth of cyclotron line | — | 0.8 ± 0.1 | — | 0.5 ± 0.1 |
| Flux ^c (1-10 keV) | 9.2 ± 0.5 | 9.2 ± 0.6 | 4.9 ± 0.2 | 4.9 ± 0.2 |
| Flux ^c (10-70 keV) | 24.5 ± 1.5 | 24.4 ± 2.0 | 9.6 ± 0.5 | 9.6 ± 1.1 |
| Flux ^c (70-130 keV) | 0.2 ± 0.1 | 0.2 ± 0.1 | — | — |
| χ^2 (dofs) | 857 (527) | 638 (524) | 863 (588) | 765 (585) |

^a : Equivalent hydrogen column density in the source direction (in 10^{22} atoms cm^{-2} units),

^b : Additional hydrogen column density (in 10^{22} atoms cm^{-2} units),

^c : Absorption corrected flux in units of 10^{-9} ergs cm^{-2} s^{-1} .

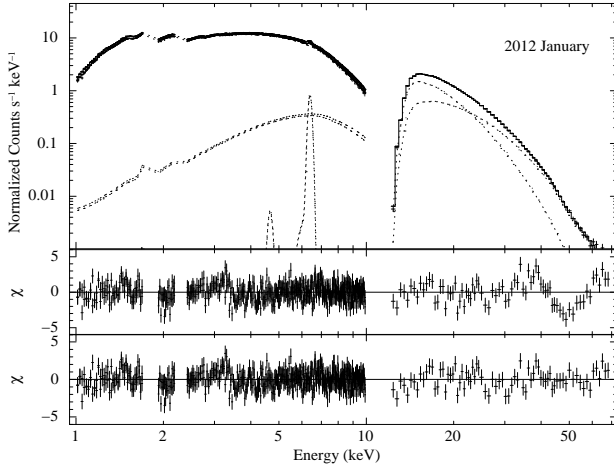


Figure 5. Energy spectrum of GX 304-1 in 1-70 keV energy range obtained with the XIS-0, XIS-3 and PIN detectors from the second *Suzaku* observation in 2012 January outburst, along with the best-fit model comprising a partial covering NPEX continuum model, a Gaussian function for iron emission line and a cyclotron absorption component. The middle and bottom panels show the contributions of the residuals to χ^2 for each energy bin for the partial covering NPEX continuum model without and with cyclotron component in the model, respectively.

procedures were followed to obtain source and background spectra, response matrices and effective area files for corresponding detectors. After appropriate background subtraction, simultaneous spectral fitting was carried out by using XSPEC v12.7 package. As the pulsar was bright during the first observation, broad-band spectral fitting was carried out in 1-130 keV range. However, data in 1-70 keV energy range were used for simultaneous fitting for second observation. The XIS spectra from 2010 August observation were binned by a factor of 4 up to 3 keV, a factor of 6 from 3 to 7 keV and

a factor of 8 from 7 to 10 keV, whereas for 2012 January observation, the XIS spectra were binned by a factor of 5 up to 10 keV. PIN spectra from both the observations were binned by a factor of 2 from 25 keV to 45 keV, a factor of 3 from 45 keV to 50 keV and a factor of 5 from 50 to 70 keV. The GSO spectra were grouped as suggested by instrumentation team. Data in 1.7-1.9 keV and 2.2-2.4 keV energy ranges were ignored from the spectral fitting due to the presence of known Si and Au edge features in the XIS spectra. All the spectral parameters except the relative normalization of detectors were tied together during the fitting.

It has been found that the phase-averaged spectra of Be/X-ray binary pulsars during outbursts have been described by power-law (e.g. GX 304-1; Maurer et al. 1982), high energy cutoff power-law (e.g. 4U 0115+63, 4U 1145-61, GX 304-1; White et al. 1983), Fermi Dirac cutoff power-law (e.g. X0331+53, A 0535+26; Tanaka 1986), NPEX (e.g. 4U 0115+63, X0331+53, Cep X-4; Makishima et al. 1999) continuum models. However, recently it has been found that while performing phase-resolved spectroscopy on data taken during X-ray outbursts of these pulsars, above models do not yield acceptable fit at all phase bins, specifically at phases of prominent and narrow absorption dips in the pulse profiles (Naik et al. 2011; Paul & Naik 2011; Naik et al. 2013 and references therein). To investigate the changes in spectral parameters at all phase bins (dip and non-dip phases of the pulse profiles), a partial covering absorption component has been added to above standard continuum models. Addition of this component to the continuum model resulted in getting acceptable fit to all phase bins and explained the cause of the narrow and prominent dips in the pulse profiles. Partial covering absorption model consists of two different power-law components with same photon index but different normalizations, being absorbed by different column densities (N_{H1} & N_{H2}), respectively (Endo et al. 2000).

In the beginning, standard continuum models such

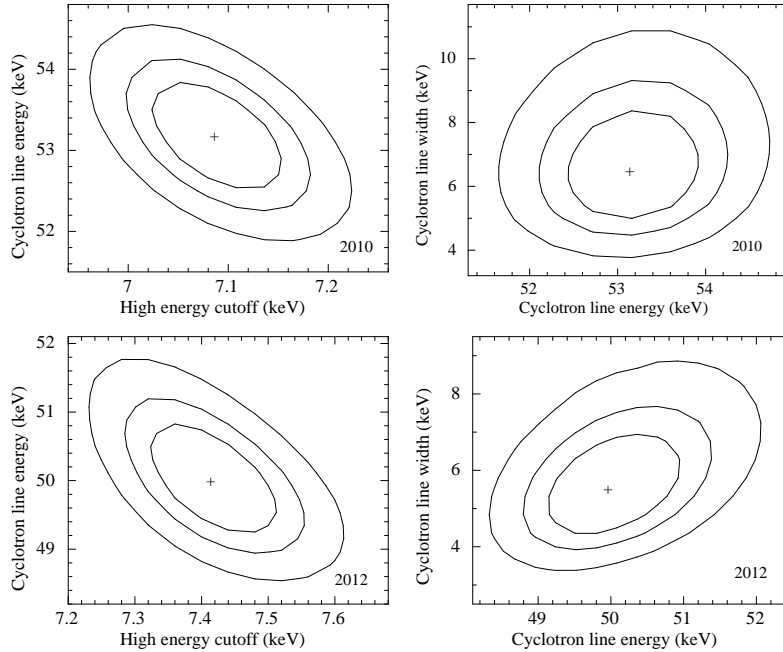


Figure 6. The χ^2 confidence contours between high energy cutoff, cyclotron line energy and width, obtained from the phase averaged spectra fitted by the partial covering NPEX model with cyclotron component during 2010 August (upper panel) and 2012 January (lower panel) *Suzaku* observations. The innermost to outermost contours represent 68%, 90% and 99% confidence levels, respectively. The “+” sign indicates the best fit values for both parameters.

as high energy cutoff power-law (HECUT; White et al. 1983), Fermi Dirac cutoff power-law (FDCUT; Tanaka 1986), NewHcut (Burderi et al. 2000), cutoff power-law, NPEX (Makishima et al. 1999) and Thermal Comptonization model (CompTT; Titarchuk 1994) were used in our spectral fitting to describe the continuum spectrum of GX 304-1. Due to the presence of narrow absorption dips in the pulse profiles of the pulsar (previous section) as seen in other Be/X-ray binary pulsars, a partial covering absorption component was added to above continuum models. Among these models, partial covering NPEX continuum model was found to fit the source spectra obtained from both the observations better than all other continuum models. We selected this model to use in phase-averaged and phase-resolved spectral analysis of both the *Suzaku* observations of GX 304-1.

The NPEX continuum model is a combination of two power-laws with positive and negative indices and a high energy cutoff. This model is an approximation of the unsaturated thermal Comptonization in hot plasma. The analytical form of NPEX model is

$$NPEX(E) = (N_1 E^{-\alpha_1} + N_2 E^{+\alpha_2}) \exp\left(-\frac{E}{kT}\right)$$

where N_1 , α_1 and N_2 , α_2 are the normalization and photon index of the negative and positive power laws, respectively. kT represents the cutoff energy in the unit of keV. The photon index of positive power law is fixed at a value of 2, representing Wien’s peak. During the spectral modeling, we found that the partial covering NPEX model described the 1-130 keV (2010 observation) and 1-70 keV (2012 observation) spectra of the pulsar well. In addition to the continuum, iron fluorescence emission line at ~ 6.4 keV

was detected in spectrum during both the observations. A weak iron emission edge like feature was found in the residual during the fitting of second observation. This was modeled by the addition of an edge component at ~ 7.7 keV in the spectral model.

An absorption like feature at ~ 54 keV was clearly seen in residuals obtained from spectral fittings of both the observations. Addition of a cyclotron absorption component (‘CYCLABS’ in *XSPEC* package) in the partial covering NPEX continuum model improved spectral fitting further with reduced χ^2 of ~ 1.5 for both the observations. The values of reduced χ^2 , though acceptable, are found to be large. Investigating the residuals in 1-10 keV range, we noticed a marginal cross calibration uncertainties present between XIS-1 (back illuminated CCD) and XIS-0 & 3 (front-illuminated CCD) spectra. While fitting the broad-band spectra without considering data from XIS-1, the values of reduced χ^2 obtained are 1.22 and 1.31 for first and second observations, respectively. Best-fit model parameters obtained from simultaneous spectral fitting of XIS-0 & 3, PIN and GSO data are given in Table 1. The energy spectra of the pulsar along with the best-fit model components are shown in Fig. 4 and 5. The middle and bottom panels in each figure show the residuals to the best-fit model without and with the addition of cyclotron absorption feature in the continuum model, respectively. The χ^2 confidence contours were plotted to check the dependence of the cyclotron line energy on high energy cutoff and cyclotron width and are shown in the top and bottom panels of Fig. 6 for first and second observations, respectively. We did not find any strong degeneracy among these spectral parameters.

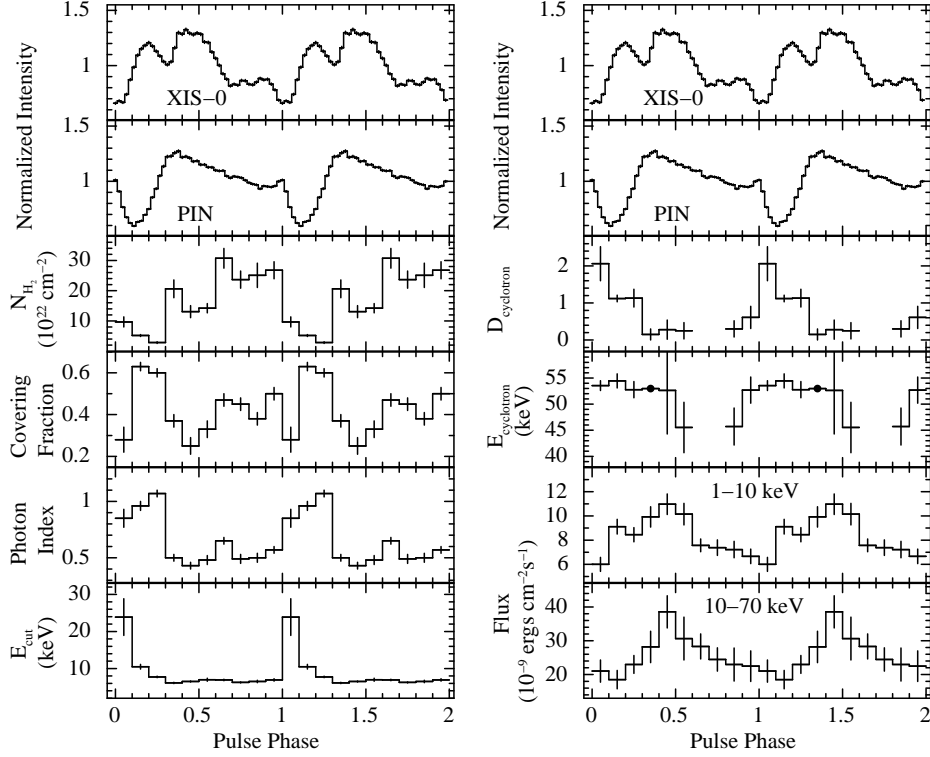


Figure 7. Spectral parameters obtained from the phase-resolved spectroscopy of GX 304-1 during the *Suzaku* observation in 2010 August. The first and second panels in both sides show pulse profiles of the pulsar in 0.5-10 keV (XIS-0) and 10-70 keV (HXD/PIN) energy ranges. The values of N_{H_2} , covering fraction, power-law photon index and cutoff energy (E_{cut}) are shown in third, fourth, fifth and sixth panels in left side, respectively. The cyclotron line parameters such as depth (third panel), line energy (fourth panel), source flux in 1-10 keV (fifth panel) and 10-70 keV (sixth panel) are shown in right side of the figure. Solid circles in the fourth panel in right side indicate that the cyclotron line energy was fixed for corresponding phase-bin at the phase-averaged value. The errors in the figure are estimated for 90% confidence level.

3.2.2 Pulse-phase-resolved spectroscopy

Pulse profiles of GX 304-1 are found to be different even when compared at same energy range from both *Suzaku* observations. Therefore, it is interesting to perform phase-resolved spectroscopy to probe the changes in spectral parameters with pulse phase and then compare with the observations at different luminosity level. As the first observation was for a relatively short exposure (~ 13 ks for HXD) compared to the second observation (~ 59 ks for HXD), phase-resolved spectroscopy was carried out by accumulating source spectra in 10 and 16 pulse-phase bins for first and second observations, respectively. Reprocessed XIS and PIN event data from both the observations were used to extract phase-resolved spectra by applying phase filter in *XSELECT* package. Data from HXD/GSO detector were not used in the phase resolved spectroscopy due to lack of sufficient hard X-ray photons in each phase bin. Background spectra and response matrices used in phase-averaged spectroscopy were also used in phase-resolved spectral fitting. Simultaneous spectral fitting was carried out on phase-resolved spectra obtained from both the observations by using partial covering NPEX continuum model along with the cyclotron absorption component and Gaussian function for the iron emission line. While fitting, the values of relative instrument normalizations, equivalent hydrogen column density (N_{H_1}) and iron emission line parameters were fixed at the corresponding values obtained from phase-averaged

spectroscopy. The width of the cyclotron absorption line was fixed at the phase averaged value to constrain the feature. Spectral parameters obtained from fitting the XIS and PIN phase resolved spectra are shown in Fig. 7 and 8 for 2010 August 13 and 2012 January 31 observations, respectively. Pulse profiles obtained from XIS-0 and PIN event data of each observation are also shown in top two panels of these figures.

During both the observations, all the spectral parameters showed significant variability with pulse-phase of the pulsar. Fig. 7 (2010 August observation) shows that the value of additional hydrogen column density (N_{H_2}) varies in $1-30 \times 10^{22} \text{ cm}^{-2}$ range over pulse phases. The value of N_{H_2} was increased from 0.3 phase and became maximum in 0.6-1.0 phase range. It can be seen that normalized intensity (XIS pulse profile; top panel) was low at 0.6 phase and remain steady before reaching the minimum value at 1.0 phase. Decrease in the normalized intensity of the pulsar during above pulse phase range and simultaneous increase in the value of N_{H_2} confirm that the plateau like feature in XIS pulse profile in 0.6-1.0 pulse phase range was due to the presence of additional absorbing material close to the pulsar. This can also explain the presence of an absorption dip in the XIS pulse profile and an increase in the N_{H_2} value in 0.3-0.4 phase range of the pulsar. As in case of N_{H_2} , the covering fraction of the additional absorption was also found to be comparatively high during the dip and plateau region. As expected, the values of power-law photon index and cutoff

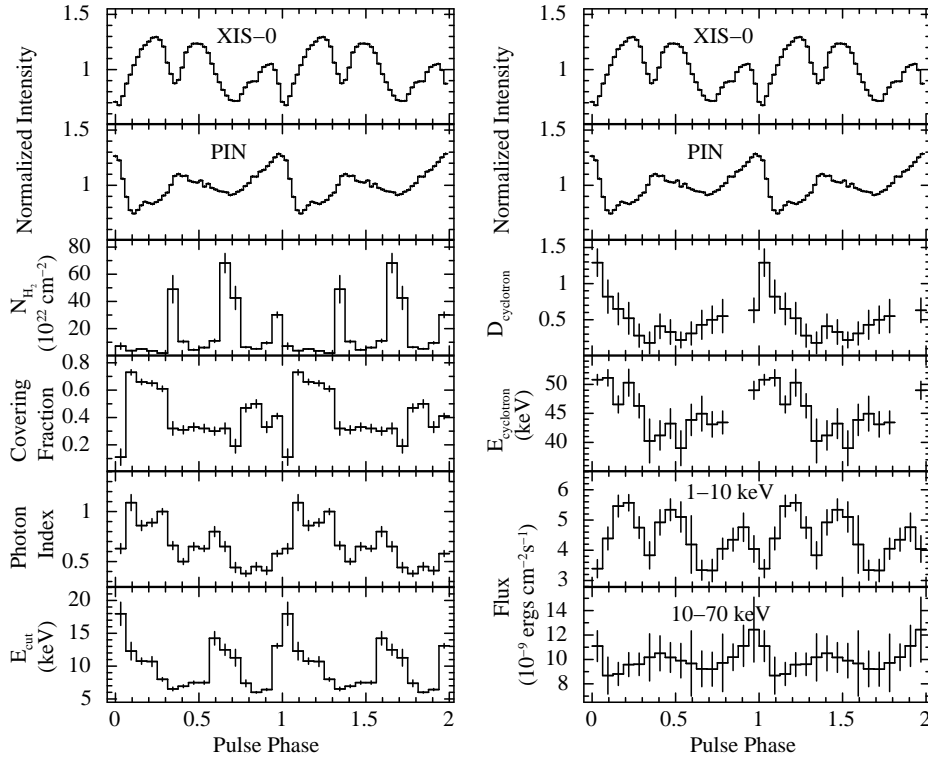


Figure 8. Spectral parameters obtained from the phase-resolved spectroscopy of GX 304-1 during the *Suzaku* observation in 2012 January. The first and second panels in both sides show pulse profiles of the pulsar in 0.5-10 keV (XIS-0) and 10-70 keV (HXD/PIN) energy ranges. The values of N_{H_2} , covering fraction, photon index and cutoff energy (E_{cut}) are shown in third, fourth, fifth and sixth panels in left side, respectively. The cyclotron line parameters such as depth (third panel), line energy (fourth panel), source flux in 1-10 keV (fifth panel) and 10-70 keV (sixth panel) are shown in right side of the figure. The errors in the figure are estimated for 90% confidence level.

energy were high during the main dip in the XIS and PIN pulse profiles. The depth of the cyclotron absorption feature was found to be variable and single peaked. The energy of cyclotron absorption feature also showed variation over the pulse phase of the pulsar. The values of both the parameters were maximum at dip phase of the pulsar and gradually decreased to minimum value in 0.5-0.8 phase range. Data gaps in third and fourth panels in second column are due to the non-detection of cyclotron features in the spectral fitting for corresponding phase-bins. The flux in 1-10 keV and 10-70 keV shows variation with pulse phase and follows the shape of pulse profile in respective energy bands.

Though the shape of XIS and PIN pulse profiles of the pulsar were significantly different during second *Suzaku* observation, the variation of spectral parameters over pulse phase was comparable. High values of absorption column density were found at phases of absorption dip in XIS pulse profile. The values of power-law photon index, cutoff energy, depth and energy of cyclotron absorption line, source flux in 1-10 keV and 10-70 keV were followed similar pattern as seen during the 2010 August *Suzaku* observation of the pulsar. Though the number of absorption dips and shape of the pulse profiles of the pulsar during both the observations were different, presence of additional matter as the cause of absorption dips in the soft X-ray profiles is supported by the findings in the present work. However, low value ($\leq 5 \times 10^{22} \text{ cm}^{-2}$) of absorption column density at ~ 0.1 -0.2 phase range (Fig. 2 & 3) suggested that the cause of absorption dip at

above phase range in the hard X-ray pulse profiles was different.

4 DISCUSSION AND CONCLUSIONS

Pulse profiles of transient X-ray binary pulsars are complex due to the presence of multiple absorption dips/features at lower energies. These absorption features are strongly energy dependent – prominent in soft X-ray pulse profiles and gradually disappear at higher energies. Complex structures or absorption dips in pulse profiles originate due to the photo-electric absorption of soft X-ray photons by matter present around the neutron star. This can be confirmed by investigating energy resolved pulse profiles and the evolution of spectral properties with pulse phases of the pulsar. Among the accretion powered X-ray pulsars, the pulse profiles of Be/X-ray binary pulsars during outbursts are found to be complex. These pulsars show regular and periodic X-ray outbursts (Type I) that are associated with the periastron passage of the neutron star. During periastron passage, the neutron star captures copious amount of matter from the circumstellar disk of the Be companion star and undergoes X-ray outbursts. Typical X-ray luminosity of the pulsar during Type I outburst is $\sim 10^{36-37} \text{ erg s}^{-1}$ (Negueruela et al. 1998). In case of GX 304-1, Type I X-ray outbursts occur at a period of 132.5 d. Using instruments with good time resolution and wide-band energy coverage capabilities onboard *Suzaku*, we carried out a detailed study of the pulsar dur-

ing two Type I outbursts. We also performed pulse-phase resolved spectroscopy of GX 304-1 to study the evolution of spectral parameters during these outbursts.

4.1 Pulse Profiles

Pulse profiles of GX 304-1 appeared to be different during 2010 August and 2012 January Type I outbursts. During 2010 August observation, the profiles were complex due to the presence/absence of peaks and dips at several pulse phases in soft and hard X-ray energy ranges. Due to this, a phase shift of ~ 0.1 was visible between the soft and hard X-ray pulse profiles (Fig. 1 & 2). However, the shape of the pulse profiles of the pulsar during 2012 January outburst were significantly different compared to 2010 August outburst. Number of absorption dips in the pulse profiles was more during 2012 observation. The strength of these dips was also prominent compared to the earlier observation. These dips were present in the pulse profiles up to higher energies unlike the 2010 August observation, where the dips were seen in the pulse profiles up to ~ 10 keV. Pulse-phase resolved spectroscopy during both the observations revealed the presence of additional matter at certain phases, causing the absorption dips in the soft X-ray pulse profiles. During 2012 observation, more number of narrow absorption dips in the pulse profiles suggest the presence of dense narrow streams of matter around the neutron star. However, during 2010 observation, relatively simpler profile with single absorption dip and a plateau phase suggests that the matter distribution around the neutron star is different and relatively simple. The luminosity of the pulsar during 2010 *Suzaku* observation was estimated to be higher ($2.3 \times 10^{37} \text{ ergs s}^{-1}$) than the 2012 *Suzaku* observation ($1 \times 10^{37} \text{ ergs s}^{-1}$). The peak luminosity of 2010 August outburst was also found to be high compare to the 2012 January outburst (first panels of Fig. 1). As both the outbursts are Type I X-ray outbursts, observed difference in the shape of the pulse profiles must be due to the difference in the subsequent mass accretion rate.

As in case of GX 304-1, another transient Be/X-ray binary pulsar EXO 2030+375 was also observed at the peaks of 2007 May and 2012 May Type-I outbursts with *Suzaku*. The pulse profiles of EXO 2030+375 during these two outbursts were significantly different (Naik et al. 2013; Naik & Jaisawal 2015). During the luminous outburst in 2007 May, the pulse profile of EXO 2030+375 consisted of several absorption dips as seen in the pulse profiles of GX 304-1 during 2012 January outburst. However, during the less intense 2012 May outburst, the pulse profiles were relatively smooth. Difference in the mass accretion rate during these two Type I outbursts was interpreted as the cause of different shape of pulse profiles in EXO 2030+375. Such type of pulse profiles with multiple dips are also seen in other Be/X-ray binary pulsars such as A0535+35 (Naik et al. 2008), GRO J1008-57 (Naik et al. 2011), 1A 1118-61 (Maitra et al. 2012 and references therein). The dips in pulse profiles of these pulsars are originated due to the absorption of emitted radiation by matter close to the neutron star. In most of the cases, the dips in the pulse profiles are seen only in soft X-rays. However, there are a few Be/X-ray pulsar in which the absorption dips are seen at same phase in the pulse profiles up to higher energy (~ 70 keV) e.g. EXO 2030+375 (Naik et al.

2013). This is interpreted as due to the presence of dense additional absorbers at various narrow pulse phase bins of the pulsar. Though, dip-like features in GX 304-1 (present work) appeared up to ~ 50 keV, the low value of additional column density at dip phases suggests that absorption is not the cause of these dips in hard X-ray pulse profiles.

Energy resolved pulse profiles of GX 304-1, obtained from both the *Suzaku* observations revealed a significant phase-shift (~ 0.35) of the main dip in profiles at energies below and above ~ 35 keV. The observed phase-shift of the main dip happened to occur at an energy close to the cyclotron absorption line energy in GX 304-1. Such type of effects e.g. phase-shifts (lags) or significant variations in pulse profiles close to the cyclotron absorption line energy are also seen in two other Be/X-ray binary pulsars such as V 0332+53 (Tsygankov et al. 2006) and 4U 0115+63 (Ferrigno et al. 2011). Using a numerical study on the effect of cyclotron resonant scattering in highly magnetized accretion powered X-ray pulsars, Schönherr et al. (2014) showed that a strong change in the pulse profile is expected at the cyclotron absorption line energy. This change is attributed to the effects of angular redistribution of X-ray photons by cyclotron resonant scattering in a strong magnetic field combined with relativistic effects. In GX 304-1, we observed a significant change in the phase of main dip in the pulse profile close to the cyclotron line energy. This detection, along with the reported results from V 0332+53 and 4U 0115+63 supports the results obtained from the numerical study of Schönherr et al. (2014).

4.2 Spectroscopy

Broad-band spectra of accretion powered X-ray pulsars are described by several continuum models such as HIGHECUT, FDCUT, cutoff power-law, NPEX, CompTT. Along with the continuum model, additional components such as absorption due to matter present in the interstellar medium, blackbody/bremsstrahlung for soft X-ray excess, Gaussian functions for emission lines and cyclotron resonance scattering features (CRSF) are also needed to explain the observed spectrum. In case of several Be/X-ray binary pulsars, a partially absorption component is being used to describe the presence of several absorption features (dips) at certain phases in the pulse profiles (Paul & Naik 2011 and references therein). Detection of CRSF in the broad-band pulsar spectrum provides direct estimation of the magnetic field of X-ray pulsars. However, studies of CRSF at different pulse phases of the pulsars can reveal important information about the magnetic field geometry around the neutron star. Therefore, broad-band spectroscopy of data obtained from the observations with high spectral capability instruments on-board *Suzaku* is an appropriate tool to understand the properties of accretion powered X-ray pulsars.

This paper reports the broad-band phase-averaged and phase-resolved spectroscopy of GX 304-1 by using two *Suzaku* observations during its Type I outbursts. The estimated values of galactic equivalent hydrogen column density in the source direction (N_{H1}) was same (within errors) during both the observations. However, the values of additional column density (N_{H2} - local to the pulsar), were found to be different during both the observations. The value of N_{H2} was high during the 2010 August observation compared

to 2012 January observation. It should be noted here that the luminosities of the pulsar during the *Suzaku* observation (Table 1) as well as at the peak (top panels of Fig. 1) of 2010 August outburst were high compared to corresponding values during 2012 January outburst. This confirms that the amount of mass accreted by the neutron star from the Be circumstellar disk during 2010 August outburst was significantly more than that during 2012 January outburst. Similar findings have also been reported for EXO 2030+275 during its Type I outbursts with significantly different luminosities (Naik et al. 2013; Naik & Jaisawal 2015). High value of N_{H_2} during more luminous Type I outbursts in Be/X-ray binary pulsars can be explained as due to significant amount of mass accreted by the neutron star from the circumstellar disk of the Be companion star.

We estimated the effect of additional column density (N_{H_2}) on the phase averaged spectrum by taking the difference in absorption corrected flux without and with N_{H_2} component. It was found that the 2010 August observation was more affected by absorption due to additional matter compared to the 2012 January observation. The flux differences were estimated to be $(1.8 \pm 0.9) \times 10^{-9}$ and $(0.4 \pm 0.3) \times 10^{-9}$ ergs cm $^{-2}$ s $^{-1}$ for 2010 August and 2012 January observations, respectively. The covering fraction which is defined as $Norm2/(Norm1+Norm2)$, where $Norm1$ and $Norm2$ are the normalizations of first and second power-law, was also found to be high during first observation. Covering fraction describes the possibility of interaction of photons with the absorbing matter which is marginally offset from the line of sight at a phase averaged solid angle of $\Omega/4\pi = Norm2/Norm1$ (Endo et al. 2000). The averaged phase solid angles ($\Omega/4\pi$) for first and second observations were estimated to be 0.47 and 0.30, respectively. This indicates that the additional absorbing matter during first observation was present relatively more closer to the neutron star that extending to a larger solid angle.

Absorption dips in the pulse profiles of Be/X-ray binary pulsars are explained as due to the presence of narrow streams of matter that are phase-locked with the neutron star. The magnetospheric radius of the pulsar can be used to constrain the location of additional absorbing matter in such narrow streams. The size of magnetosphere of the pulsar depends on the mass accretion rate and the strength of the magnetic field (Mushtukov et al. 2015a and references therein) through the relation

$$R_m = 2.6 \times 10^8 M^{1/7} R_6^{10/7} B_{12}^{4/7} L_{37}^{-2/7} \text{ cm} \quad (1)$$

Using standard values of mass and radius of canonical neutron stars and the observed luminosities of GX 304-1 in above equation, the magnetospheric radii were estimated to be ~ 5100 and 6300 km during first and second observations, respectively. This confirmed that the pulsar magnetosphere was relatively small during the first observation. Therefore, the streams of additional matter were present within the magnetosphere and found to be closer to the pulsar during the first *Suzaku* observation.

Pulse-phase resolved spectroscopy of GX 304-1 during two Type I outbursts showed the presence of narrow streams of matter (higher value of N_{H_2}) at several pulse phase ranges. The presence of such streams of matter are interpreted as the cause of absorption dips detected in soft X-ray pulse profiles of the pulsar. Several such dips are seen

in the pulse profiles of Be/X-ray binary pulsars during X-ray outbursts. Density and opacity of matter in these narrow streams decides the energy dependence of the dips in the pulse profiles of these pulsars. During both the observations, pulse-phase variation of covering fraction was found to be similar. We suggest that the geometry or distribution of absorbing matter around the pulsar is probably similar during both observations but at different locations.

4.3 Cyclotron line in GX 304-1

Cyclotron absorption line or CRSF was clearly detected in the spectra of GX 304-1 during both the observations and was described with pseudo-Lorentzian function (CYCLABS) in the continuum model. These are absorption like features which appear in hard X-ray spectrum (~ 10 -100 keV) through the resonant scattering of the photons with electrons in strong magnetic field ($\sim 10^{12}$ G) near the poles of the neutron star. The cyclotron line energy is related with the magnetic field through the relation $E_{cyc} = 11.6 B_{12} \times (1+z)^{-1}$ (keV) or 12-B-12 rule, where B_{12} is the magnetic field in the unit of 10^{12} G and z is the gravitational red-shift. Detection of CRSF in the pulsar spectrum, therefore, provides the direct measurement of the magnetic field of the neutron star. Though, CRSF was already detected in GX 304-1 (Yamamoto et al. 2011), *Suzaku* observations at different source intensities provide an opportunity to investigate the luminosity dependence of the cyclotron line energy. The cyclotron feature was detected at ~ 53 and 50 keV during 2010 August and 2012 January *Suzaku* observations, respectively. The observed cyclotron absorption line energies are not significantly different. However, it shows a positive dependence on the pulsar luminosity, as seen in Her X-1 (Staubert et al. 2007). In some other cases such as 4U 0115+63 (Nakajima et al. 2006; Tsygankov et al. 2007), and V 0332+53 (Tsygankov et al. 2010), a negative correlation is observed between the luminosity of pulsar and the cyclotron absorption line energy.

Attempts have been made to explain the observed positive and negative correlation between pulsar luminosity and the cyclotron line energy. A negative correlation is expected in super-critical regime where the source luminosity is higher than the critical luminosity (Becker et al. 2012; Mushtukov et al. 2015a). Above critical luminosity, density of infalling matter becomes so high that the particles start interacting and decelerating through the formation of a radiation-pressure dominated shock above the neutron star surface. Cyclotron scattering features most likely occur closer to the shock region. With increasing luminosity, the shock height drift upwards in the accretion column where relatively low strength of magnetic field produces cyclotron feature at lower energy. It explains negative correlation as observed in 4U 0115+63 and V 0332+53. However, the positive correlation is predicated for a sub-critical regime e.g. below critical luminosity. The pressure of accreting matter in this regime pushes hydrodynamical shock closer to the neutron star surface where increase in the strength of magnetic field with luminosity results a positive correlation between the cyclotron line energy and luminosity (Staubert et al. 2007), as seen in Her X-1 and GX 304-1. The 1-70 keV luminosity of GX 304-1 during first and second *Suzaku* observations was estimated to be 2.3×10^{37} and 1×10^{37} ergs s $^{-1}$, respec-

tively, which lies in the sub-critical regime (Mushtukov et al. 2015a) and expected to show a positive correlation with cyclotron line energy.

Poutanen et al. (2013) and Nishimura (2014) have proposed alternate models to describe the dependence of cyclotron absorption line energy on the source luminosity. In these models, it is argued that the formation of cyclotron line in direct spectrum is questionable due to the large gradient of magnetic field strength along line forming region in the accretion column. However, cyclotron line (CRSF) can be formed in the reflected radiation from the surface of the neutron star where magnetic field gradient is relatively small (Poutanen et al. 2013). It is widely believed that the accretion column height is linearly dependent on source luminosity ($>10^{37}$ ergs s^{-1}) or accretion rate. At higher luminosity, larger area on neutron star surface (from the poles with strong magnetic field towards equator with weak field strength) is expected to be illuminated for cyclotron interactions. This explains the observed anti-correlation between cyclotron line energy and luminosity, as seen in V 0332+53. However, Nishimura (2014) described the observed correlations by considering the changes in polar emission region, direction of photon propagation and the shock height. The negative correlation was interpreted in terms of shock region displacement whereas the positive correlation was explained by using the changes in beam pattern. In case of GX 304-1 (present work), the cyclotron absorption line width, depth and ratio of line width and energy (W/E_{cyl}) show positive correlation with luminosity. The observed positive correlation between the cyclotron line energy and luminosity in GX 304-1, therefore, can be explained as due to the change in beam pattern, as described by Nishimura (2014). Alternatively, Mushtukov et al. (2015b) discussed the positive luminosity dependence of sub-critical X-ray pulsars like GX 304-1 by studying the changes of plasma velocity profile in line-forming region under influence of radiation pressure from the hot-spot. The cyclotron line energy at a luminosity was determined by corresponding redshift from velocity profile at a given height. This model successfully predicts the positive luminosity correlation of cyclotron line energy for pulsars like GX 304-1 along with cyclotron line width dependence on luminosity and pulse phase variation of cyclotron line parameters, which were not being discussed in Nishimura (2014).

Investigation of the change in cyclotron parameters with pulse phase of the pulsar provides important evidences to understand the emission geometry as well as the magnetic field mapping around the neutron star. A comparative study of these parameters at different intensity levels during several outbursts can also yield information about the changes in emission or accretion column geometry. Pulse-phase resolved spectroscopy of cyclotron absorption line is one of the interesting results of this work. During both *Suzaku* observations of the pulsar, cyclotron energy and depth were found significantly variable with pulse-phase. Change in cyclotron line parameters with pulse phase has also been seen in other X-ray pulsars such as Cen X-3 (Burderi et al. 2000), GX 301-2 (Kreykenbohm et al. 2004), 1A 1118-61 (Maitra et al. 2012), A 0535+26, XTE J1946+274, 4U 1907+09 (Maitra & Paul 2013), V 0332+53 (Lutovinov et al. 2015) and Cep X-4 (Jaisawal & Naik 2015) with ~ 10 -30% variation in cyclotron energy.

The cyclotron line energy for GX 304-1 was found variable with phase up to 17% and 24% for first and second *Suzaku* observations, respectively. However, the cyclotron line depth showed phase dependence within a factor of ~ 2.5 for both observations. Various simulations were performed to study the dependence of the cyclotron line on pulsar phases, assuming certain sets of rule and geometry in line forming region (Schönherr et al. 2007; Mukherjee & Bhattacharya 2012). These studies predicated that 10-30% variation in cyclotron energy with phases can be resulted due to effects of viewing angle of accretion column or emission region. However, more than 30% changes in cyclotron energy is contributed by distortion in the magnetic field geometry. In GX 304-1 (present work), cyclotron energy is found to be variable within 24% for both observations which can be explained as effects of viewing angle or local distortion in the magnetic field in line forming region. We found that the cyclotron energy and depth for both observations were peaking around the 1.0-1.1 (or 0.0-0.1) phase range, which lies closer to the peak of pulse profiles at ≥ 35 keV. This result supports the effect of cyclotron resonance scattering on beaming pattern that changes the shape of the pulse profiles.

In summary, the timing and spectral properties of GX 304-1 were presented by using *Suzaku* observations during Type I outbursts. Absorption dips were detected in the pulse profiles at soft X-rays. These dips were originated due to obscuration/absorption of X-ray photons with narrow streams of accretion flow at certain pulsar phases. The shape of pulse profiles was significantly changed at ≥ 35 keV e.g. close to the cyclotron line energy. Significant pulse phase dependence of cyclotron line was explained as the effects of viewing angle or the role of complicated magnetic field of the pulsar.

ACKNOWLEDGMENTS

We sincerely thank the referee for his/her valuable comments and suggestions which improved the paper significantly. The research work at Physical Research Laboratory is funded by the Department of Space, Government of India. The authors would like to thank all the members of the *Suzaku* for their contributions in the instrument preparation, spacecraft operation, software development, and in-orbit instrumental calibration. This research has made use of data obtained through HEASARC Online Service, provided by the NASA/GSFC, in support of NASA High Energy Astrophysics Programs.

REFERENCES

- Becker P., Klochkov D., Schönherr G., et al. 2012, A&A, 544, A123
- Bradt H. V., Clark G. W., Dower R., Doxsey R., Hearn D. R., Jernigan J. G., et al. 1977, Nature, 269, 21
- Burderi L., Di Salvo T., Robba N. R., La Barbera A., Guainazzi M., 2000, ApJ, 530, 429
- Corbet R. H. D., Smale A. P., Menzies J. W., Branduardi-Raymont G., Charles P. A., et al., 1986, MNRAS, 221, 961
- Devasia J., James M., Paul B., Indulekha K., 2011, MNRAS, 417, 348
- Endo T., Nagase F. and Mihara T., 2000, PASJ, 52, 223

- Ferrigno C., Falanga M., Bozzo E., Becker P. A., Klochkov D., Santangelo A., 2011, *A&A*, 532, A76
- Forman W., Jones C., Cominsky L., Julien P., Murray S., et al. 1978, *ApJS*, 38, 357
- Giacconi R., Murray S., Gursky H., Kellogg E., Schreier E., et al. 1974, *ApJS*, 27, 37
- Haefner R., 1988, *Inf. Bull. Var. Stars*, 3260, 1
- Jaisawal G. K. and Naik S., 2015, *MNRAS*, 453, L21
- Klochkov D., Doroshenko V., Santangelo A., Staubert R., Ferrigno C., et al. 2012, *A&A*, 542, L28
- Koyama K. et al., 2007, *PASJ*, 59, 23
- Kreykenbohm I., Wilms J., Coburn W. et al., 2004, *A&A*, 427, 975
- Krimm H. A., et al., 2010, *Astron. Telegram*, 2538, 1
- Lutovinov A. A., Tsygankov S. S., Suleimanov V. F. et al., 2015, 448, 2175
- Maitra C., Paul B., Naik S., 2012, *MNRAS*, 420, 2307
- Maitra C. & Paul B., 2013, 771, 96
- Makishima K., Mihara T., Nagase F., Tanaka Y., 1999, *ApJ*, 525, 978
- Manousakis A., et al. 2008, *Astron. Telegram*, 1613
- Mason K. O., Murdin P. G., Parkes G. E., Visvanathan N., 1978, *MNRAS*, 184, 45P
- Maurer G. S., Johnson W. N., Kurfess J. D., Strickman M. S., 1982, *ApJ*, 254, 271
- Malacaria C., Klochkov D., Santangelo A., & Staubert R., 2015, *A&A*, 581, 121
- McClintock J. E., Ricker G. R., Lewin W. H. G., 1971, *ApJ*, 166, L73
- McClintock J. E., Rappaport S. A., Nugent J. J., Li F. K., 1977, *ApJ*, 216, L15
- Mihara T., et al. 2010, *Astron. Telegram*, 2779
- Mitsuda K. et al., 2007, *PASJ*, 59, 1
- Mukherjee D., & Bhattacharya D., 2012, *MNRAS*, 420, 720
- Mushtukov A. A., Suleimanov V. F., Tsygankov S. S. and Poutanen J., 2015a, *MNRAS*, 447, 1847
- Mushtukov A. A., Tsygankov S. S., Serber A. V., Suleimanov V. F., Poutanen J., 2015b, *MNRAS*, 454, 2714
- Naik S., Dotani T., Terada Y., et al. 2008, *ApJ*, 672, 516
- Naik S., Paul B., Kachhara C., Vadawale S. V., 2011, *MNRAS*, 413, 241
- Naik S., Maitra C., Jaisawal G. K., Paul B., 2013, *ApJ*, 764, 158
- Naik S. & Jaisawal G. K., 2015, *RAA*, 15, 537
- Nakajima M., Mihara T., Makishima K., Niko H., 2006, *ApJ*, 646, 1125
- Negueruela I., Reig P., Coe M. J., & Fabregat J., 1998, *A&A*, 336, 251
- Nishimura O., 2014, *ApJ*, 781, 30
- Parkes G. E., Murdin P. G., Mason K. O., 1980, *MNRAS*, 190, 537
- Paul B. & Naik S., 2011, *Bull. Astron. Soc. India*, 39, 429
- Pietsch W., Oegelman H., Kahabka P., Collmar W., Gottwald M., 1986, *A&A*, 163, 93
- Priedhorsky W. C., Terrell J., 1983, *ApJ*, 273, 709
- Postnov K. A., Mironov A. I., Lutovinov A. A., Shakura N. I., Kochetkova A. Yu., Tsygankov S. S., et al. 2015, *MNRAS*, 446, 1013
- Poutanen J. et al., 2013, *ApJ*, 777, 115
- Schönherr G., et al. 2007, *A&A*, 472, 353
- Schönherr G., et al. 2014, *A&A*, 564, 8
- Staubert R., Shakura N. I., Postnov K., et al. 2007, *A&A*, 465, L25
- Sugizaki M., Yamamoto T., Mihara T., Nakajima M., & Makishima K., 2015, *PASJ*, 67, 73
- Takahashi T. et al., 2007, *PASJ*, 59, 35
- Tanaka Y., 1986, in *Proc. IAU Colloq. 89, Vol. 255, Radiation Hydrodynamics in Stars and Compact Objects*, ed. D. Mihalas & K.-H. A. Winkler
- Titarchuk L., 1994, *ApJ*, 434, 313
- Tsygankov S. S., Lutovinov A. A., Churazov E. M., & Sunyaev R. A., 2006, *MNRAS*, 371, 19
- Tsygankov S. S., Lutovinov A. A., Churazov E. M., & Sunyaev R. A., 2007, *Astron. Lett.*, 33, 368
- Tsygankov S. S., Lutovinov A. A., & Serber A. V., 2010, *MNRAS*, 401, 1628
- Yamamoto T. et al., 2009, *Astron. Telegram*, 2297, 1
- Yamamoto T., Sugizaki M., Mihara T., Nakajima M., Yamaoka K., et al. 2011, *PASJ*, 63, 751
- Yamamoto T., et al., 2012, *Astron. Telegram*, 3856, 1
- White N. E., Swank J. H. & Holt S. S., 1983, *ApJ*, 270, 711